Fluorescence Quenching of Reconstituted NCD-4-Labeled Cytochrome *c* Oxidase Complex by DOXYL-Stearic Acids[1]

Siegfried M. Musser, Randy W. Larsen,* and Sunney I. Chan
Arthur Amos Noyes Laboratory of Chemical Physics, California Institute of Technology, Pasadena, California 91125 USA

ABSTRACT It has been known for some time that dicyclohexylcarbodiimide (DCCD) inhibits the proton translocation function of the cytochrome *c* oxidase complex (CcO) and that there is one major site in subunit III which is modified upon reaction with DCCD (Glu-90 for the bovine enzyme). We have examined the reaction of bovine CcO with *N*-cyclohexyl-*N'*-(4-dimethylamino-α-napthyl)carbodiimide (NCD-4), a fluorescent analog of DCCD. NCD-4 labeling of CcO is strongly inhibited by DCCD implicating Glu-90 of subunit III as the site of chemical modification by NCD-4. The fluorescence of reconstituted NCD-4-labeled bovine CcO is strongly quenched by hydrophobic nitroxides, whereas hydrophilic nitroxides and iodide ions have a reduced quenching ability. It is concluded that the Glu-90 of subunit III resides near the protein-lipid interface of the membrane spanning region of the enzyme. Different quenching abilities of 5-, 7-, 10-, 12-, and 16-4,4-dimethyl-3-oxazolinyloxy-stearic acids suggest that the NCD-4 label is located in the membrane bilayer in the region near the middle of the hydrocarbon tail of stearic acid. In light of these results, it is unlikely that Glu-90 is part of a proton channel that is associated with the proton pumping machinery of the enzyme but the outcome of this study does not eliminate an allosteric regulatory role for this residue.

INTRODUCTION

The cytochrome *c* oxidase complex (CcO) is the terminal electron transport protein in the mitochondria of eukaryotes and the plasma membrane of some prokaryotes. In mammals, the enzyme is an integral membrane protein consisting of 12–13 different subunits and an assortment of metals including copper, iron, zinc, and magnesium. Although the enzyme exists as a dimer under physiological conditions, the functional unit appears to be the monomer. Each monomer contains four redox active metal centers: two heme A moieties (cytochrome *a* and cytochrome a_3), and two copper ions (Cu_A and Cu_B). It is generally agreed that cytochrome *a* and Cu_A mediate the electron transfer from ferrocytochrome *c* to the binuclear center (cytochrome a_3 and Cu_B) where the reduction of dioxygen to water occurs. Subunit I contains the two heme A's and Cu_B; Cu_A resides in subunit II.

CcO exploits the sidedness of the membrane to convert part of the redox-free energy of dioxygen reduction into a proton electrochemical gradient across the membrane. It accomplishes this feat in two ways. In the scalar reaction, reducing equivalents from ferrocytochrome *c* and the protons consumed by the reduction of dioxygen are taken from opposite sides of the membrane. In the vectorial reaction, protons are actively transported against a protonmotive force. It is well established that CcO pumps up to four protons for each molecule of dioxygen reduced hence a stoichiometry of ~1 H^+/e^- (Wikström, 1977; Casey et al., 1979a; Sigel and Carafoli, 1980; van Verseveld et al., 1981; Proteau et al., 1983). From thermodynamic considerations, proton translocation can only result from the last two electron transfers to the binuclear center (Chan and Li, 1990; Babcock and Wikström, 1992). Wikström (1989) has confirmed this expected result by showing that the last two electrons cause the pumping of four protons and that the proton translocation ratio for the last two electrons of the dioxygen reduction cycle must be 2 H^+/e^-. The relaxation of the proton gradient formed by CcO and other proteins in the respiratory chain is coupled to ATP synthesis by the ATP synthase (for reviews see Brunori et al. (1987), Prochaska and Fink (1987), Malmström (1990), Saraste (1990), Kadenbach et al. (1991), Müller and Azzi (1991), and Buse and Steffens (1991)).

In recent years, there has been considerable interest in the molecular mechanism of proton translocation in CcO and the redox linkage involved in this process. Redox linkage refers to the coupling of the downhill electron transfer reaction to the active transport of protons across the osmotic barrier. In direct coupling, the ligands of a redox center become protonated and subsequently deprotonated at some point during

Received for publication 6 May 1993 and in final form 23 August 1993.

*Present address: Department of Chemistry, University of Hawaii, Honolulu, HI 96822.

Address reprint requests to Dr. Sunney I. Chan.

[1] A portion of this work was presented at the 1992 ASBMB-Biophysical Society joint annual meeting (*FASEB J.* 1992, 61:A1099. Abstr.). Contribution No. 8651 from the Division of Chemistry and Chemical Engineering, California Institute of Technology, Pasadena, CA.

Abbreviations used: CcO, cytochrome *c* oxidase complex; DCCD, dicyclohexylcarbodiimide; NCD-4, *N*-cyclohexyl-*N'*-(4-dimethylamino-α-napthyl)carbodiimide; DOXYL-, 4,4-dimethyl-3-oxazolinyloxy-; NCD-4-CcO, NCD-4 labeled CcO; K-Phos, K_2HPO_4/KH_2PO_4 buffer; Brij-35, polyoxyethylene(23) lauryl ether; TEMPO, 2,2,6,6-tetramethyl-1-piperidine-*N*-oxyl; SDS, sodium dodecyl sulfate; PAGE, polyacrylamide gel electrophroesis; Tris-HCl, tris(hydroxymethyl)aminomethanehydrochloride; Tris-base, tris(hydroxymethyl)aminomethane; CCCP, carbonyl cyanide *m*-chlorophenyl hydrozone; CL, cardiolipin; PC, L-α-phosphatidylcholine; PE, L-α-phosphatidylethanolamine; RCR, respiratory control ratio; COVs, CcO vesicles; NCD-4-COVs, NCD-4-CcO vesicles; EPR, electron paramagnetic resonance; NCCD, *N*-(2,2,6,6-tetramethylpiperidyl-1-oxyl)-*N'*-cyclohexylcarbodiimide; Na-Phos, Na_2HPO_4/NaH_2PO_4 buffer; NMR, nuclear magnetic resonance.

0006-3495/93/12/2348/12 $2.00

the oxidation-reduction cycle of the metal. A number of directly coupled models have been proposed for the mechanism of redox linkage (Babcock and Callahan, 1983; Gelles et al., 1986; Mitchell, 1987, 1988; Woodruff et al., 1991; Larsen et al., 1992). Models of indirect coupling also have been proposed (Wikström, 1988; Mitchell et al., 1985). In indirect coupling, the redox state of the metal centers influences the conformational state of the proton translocating elements at some distant location in the protein.

A number of investigators have raised the possibility that some of the indirectly coupled proton translocating elements of the proton pump might reside in subunit III (Casey et al., 1980; Thompson et al., 1985; Prochaska and Reynolds, 1986; Prochaska and Fink, 1987). It has been known for some time that reaction of the enzyme with DCCD, which modifies Glu-90 of subunit III (bovine numbering), or removal of subunit III by a variety of methods results in inhibited proton translocation (Casey et al., 1979b, 1980; Azzi et al., 1981, Prochaska et al., 1981; Brunori et al., 1985; Pütter et al., 1985; Sarti et al., 1985; Thelen et al., 1985; Thompson et al., 1985; Finel and Wikström, 1986; Prochaska and Reynolds, 1986; Li et al., 1988; Haltia et al., 1991). There are at least two possible interpretations of these observations. One interpretation is that part or all of the proton translocating elements of the proton pump are located in subunit III. Alternatively, it has been hypothesized that all the proton translocating elements of the pump are located in subunits I and II (Haltia et al., 1991). In this scenario, subunit III would play a role in modulating the allosteric interactions between subunits I and II in order to accomplish the redox linkage and to vary the proton to electron stoichiometry. The percentage of inhibition of proton translocation by DCCD seems to correlate almost perfectly with the percentage of protein labeled by DCCD (Casey et al., 1980; Prochaska et al., 1981) suggesting that Glu-90 plays at least some role in the mechanism of proton pumping in CcO. However, point mutations of the *Paracoccus denitrificans* enzyme indicate that Glu-90 is not required for full proton pumping activity (Haltia et al., 1991). Although deletion of the subunit III gene in *P. denitrificans* results in decreased cytochrome *c* oxidizing activity (<5% of wild-type as measured in spheroplasts) (Haltia et al., 1991) and defective assembly of CcO (Haltia et al., 1989, 1991) indicating that subunit III plays an important role in the biogenesis of CcO, identical proton pumping activity is observed in the subunit III deletion mutant further arguing against a role for subunit III in proton translocation (Haltia et al., 1991). We question this result, however, because the low activity of the mutant enzyme should make turnover comparable to the rate of protonic leaks, thus predicting a noticeable decrease in proton pumping efficiency (i.e., lower respiratory control). In addition, we find it difficult to accept that a defectively assembled enzyme complex should have lower electron transfer activity yet full proton pumping activity.

There exist no data to exclude a regulatory role for subunit III, however; such a regulatory role has been postulated by many investigators (Brunori et al., 1985, 1987; Pütter et al., 1985; Sarti et al., 1985; Wikström and Casey, 1985; Finel and Wikström, 1986; Prochaska and Fink, 1987). If so, DCCD modification of Glu-90 may modify the tertiary folding of this subunit which in turn may have deleterious effects on its ability to exert control over the redox linkage. The allosteric regulation might even involve Glu-90 more directly if this residue participates in a salt bridge. Such interactions might lead to a lowering of the proton to electron stoichiometry with increasing membrane potential. Since proton to electron ratios are determined by extrapolation to zero membrane potential, it is not surprising that a modulating effect of subunit III has never been reported. In order to better delineate the possibility of subunit III as an allosteric effector, it is first necessary to obtain some idea of the location of Glu-90 within the protein as a whole. This paper describes the use of a fluorescent probe to try to locate Glu-90 of subunit III with respect to the membrane bilayer and the surface of the protein.

A decade ago, Chadwick and Thomas (1983) demonstrated that *N*-cyclohexyl-*N'*-(4-dimethylamino-α-napthyl)-carbodiimide (NCD-4) can be used as a fluorescent probe for DCCD binding sites in proteins with their work on the sarcoplasmic reticulum (Ca^{2+} + Mg^{2+})-ATPase. NCD-4 is a useful probe in that the starting material is nonfluorescent, yet both the protein adduct (an acylurea) and the side product of the reaction (a urea) are fluorescent. These two potential products (see scheme in Fig. 1) are readily distinguished by different fluorescent maxima (Table 1). Pringle and Taber (1985) have used NCD-4 and a series of spin-labeled stearic acids to show that the major carbodiimide binding site on the mitochondrial proton channel of the bovine F_0F_1 ATPase is fairly deeply buried within the membrane. In this work, Pringle and Taber assumed a 4–6 Å interaction distance for nitroxide quenching of fluorophores (Green et al., 1973). More recent data by Abrams and London (1992) indicate, however, an interaction distance of 11–15 Å for the quenching of fluor-

TABLE 1 Fluorescence emission maxima of NCD-4 derivatives in various solvents at 23°C*

	Emission wavelength (nm)‡		
NCD-4-derivative	Hexane	Ethanol	Ethanol/H_2O (1:1, v/v)
N-Acetylurea	398	425 (430)‖ ϕ = 0.06¶	440
Urea	—§	460 (467)‖ ϕ = 0.58¶	473
O-Phenylisourea	435	452	465

* Fluoresence properties of NCD-4 (adapted from Chadwick and Thomas (1983). NCD-4-acylurea is the adduct with the protein (Fig. 1); NCD-4-acetylurea is the model compound formed by reaction of NCD-4 with acetic acid.

‡ Excitation was at 330 nm.

§ NCD-4 urea proved too insoluble in hexane for spectral measurements.

‖ Values in parentheses represent corrected emission maxima.

¶ ϕ = quantum yield.

ophores by spin-labeled lipids. In support of the larger interaction, others have shown that in the case of covalent fluorophore-nitroxide conjugates, the interaction distance for nitroxide quenching is as large as 12 Å (Green et al., 1990) and significant quenching occurs over a separation distance of up to 20 Å (Matko et al., 1990). Since the cross section of a transmembrane α-helix including the sidechains is on the order of 10 Å, any appreciable quenching of the fluorophore in fluorophore labeled protein complexes by spin-labeled lipids or fatty acids indicates that the fluorescent label is on or near the surface of the protein at the protein-lipid interface of the membrane spanning region of the enzyme. The goal of the present study is to apply the Pringle and Taber methodology to the Glu-90 question in CcO.

MATERIALS AND METHODS

Materials

Beef heart CcO was isolated by the method of Hartzell and Beinert (1974). Enzyme concentrations were determined by using the reduced-minus-oxidized difference spectrum at 605 nm ($\Delta\epsilon_{605}^{red\text{-}ox} = 24\ mM^{-1}\ cm^{-1}$). Enzyme preparations were stored at −80°C in 25 mM, pH 7.8, K-Phos and 0.5 or 0.1% Brij-35 until ready for use. Native CcO had an activity of ~390 s^{-1} in 10 mM, pH 6.0, K-Phos, 100 mM KCl and 0.05% dodecyl-β-D-maltoside with an initial ferrocytochrome *c* concentration of 50 μM.

Unless otherwise described below, chemicals were reagent grade, were obtained from commercial suppliers and were used without further purification. NCD-4 and 5-, 7-, and 12-DOXYL-stearic acids were obtained from Molecular Probes; 10-DOXYL-stearic acid and TEMPO were from Aldrich; and 16-DOXYL-stearic acid was from Molecular Probes or Aldrich. Carbonyl cyanide *m*-chlorophenylhydrozone (CCCP) was obtained from Calbiochem; cytochrome *c* (type VI), and 4-amino-TEMPO were from Sigma; valinomycin was from Sigma or Calbiochem. Lipids from Sigma were as follows: bovine heart cardiolipin (CL); synthetic dioleoyl L-α-phosphatidylcholine (PC), ~99%; and synthetic dioleoyl L-α-phosphatidylethanolamine (PE), ~99%. Cholic acid (Sigma) was twice recrystallized from water/ethanol (1:1, v/v) and stored at 4°C and pH 7.6 as a 20% stock solution of the potassium salt. DEAE Bio-gel was from Bio-Rad; DE-52 beads were from Whatman, and Sephadex G-25 and G-100 were from Sigma.

Spectroscopic Methods

Optical absorption spectra and kinetic measurements were obtained with an HP8452 diode array UV/Vis spectrophotometer. EPR spectra were recorded using a Varian E-line Century Series X-band spectrometer; protein samples were at liquid nitrogen temperature and spin-labels were at room temperature. Steady-state fluorescence spectra were recorded on an SLM 4800 spectrofluorimeter equipped with a SMC-210 monochromater controller and SE-480–485 electronics (SLM Instruments) which were interfaced to an IBM XT computer. Scattering data were obtained at 90° to a Spectra-Physics series 2000 Argon laser beam (488 nm) using a Malvern System 4700c sub-micron particle analyser interfaced to a Malvern PC 6300.

NCD-4 Modification of CcO

NCD-4-modified CcO (NCD-4-CcO) was prepared as follows. To a 5 μM solution of CcO in 10 mM pH 7.4 K-Phos, 0.1% Brij-35 was added a 100-fold molar excess of NCD-4 from a 100 mM ethanol stock solution. The mixture was incubated at 4°C for 18 or 24 h and then centrifuged at 20,000 *g* for 10 min to remove the precipitated urea. The supernatant was concentrated to about 100 μM using Centricon-100s (Amicon). The concentrated NCD-4-labeled protein was then applied to a DEAE or DE-52 column equilibrated with 10 mM pH 7.4 K-Phos, 0.1% Brij-35 (low salt). After washing with this buffer (to remove the NCD-4-urea), the salt concentration was increased to 100 mM KCl (high salt) for elution of the protein. The protein was concentrated (as above), diluted to remove 90% of the KCl, and concentrated again, the final concentration being accurately determined using $\Delta\epsilon_{605}^{red\text{-}ox} = 24\ mM^{-1}\ cm^{-1}$. For the DCCD inhibition experiments, the enzyme was first incubated with a 100- or 500-fold molar excess of DCCD (from a 100 mM ethanol stock solution) for 18 h at 4°C; after the addition of a 100-fold excess of NCD-4, the incubation was continued for another 18 h. Removal of DCCD- and NCD-4-ureas was accomplished by anion exchange chromatography as described above.

NCD-4-labeled subunits were determined by sodium dodecyl sulfate-polyacrylamide gel electrophoresis (SDS-PAGE). CcO samples were dissociated using 250 mM pH 6.2 Tris-HCl, 8 M urea, 3.3% 2-mercaptoethanol, 5% SDS at room temperature for 1 h and run on a LKB2001 vertical electrophoresis unit using a 7%/0.19% (acrylamide/bisacrylamide) stacking gel, a 14%/0.37% running gel, and a running buffer of 20 mM pH 8.4 Tris-base, 240 mM glycine, and 0.1% SDS. Gels were first photographed under UV illumination to observe the NCD-4 fluorescence; staining with Coomassie Blue allowed identification of the subunits.

Reconstitution of CcO

CcO vesicles (COVs) were formed by the cholate dialysis technique (Hinkle et al., 1972). PC/PE/CL lipid mixtures (2:2:1, w/w) were brought to near dryness under a stream of nitrogen and residual solvent was removed by vacuum desiccation overnight. The dried lipids were made to a concentration of 25 mg/ml in 93 mM pH 7.4 K-Phos, 1.5% K-Cholate, and sonicated to clarity using a model W-375 tip sonicator from Heat Systems-Ultrasonics, Inc. After cooling for 10 min, 3.5 ml of the sonicated lipids were mixed with CcO and 100 mM pH 7.4 K-Phos to a final volume of 5.0 ml and CcO concentration of 2 μM. The protein-lipid solution was then incubated on ice for 15 min and thereafter centrifuged at 20,000 *g* for 30 min at 4°C. The supernatant was dialyzed (Spectra/Por 4 tubing; 12–14,000 molecular weight cutoff) for at least 22 h at 4°C against 75 volumes of 100 mM pH 7.4 K-Phos with three changes of buffer. After dialysis, the vesicles were centrifuged at 20,000 *g* for 40 min at 4°C, and the supernatant was stored at 4°C until use.

Respiratory control ratios (RCRs) of the COVs were determined as follows. Cytochrome *c* stock freshly reduced with sodium dithionite was passed through a 1.5 × 16 cm Sephadex G-25 column equilibrated with 1 mM pH 7.4 K-Phos to remove the excess dithionite. The activity of the COVs was monitored by following the cytochrome *c* absorption at 550 nm as a function of time after the addition of 4 μl vesicles to a 2-ml solution of 40 μM ferrocytochrome *c*, 8 μM CCCP, 7 μM valinomycin, and 1 mM pH 7.4 K-Phos in a stirred cuvette. The initial slope was determined and compared with that of an equivalent kinetics run with no ionophores to give the RCR. Typical RCRs for the COVs were between 2 and 3; respiratory control was almost completely lost in the case of the NCD-4-CcO vesicles (NCD-4-COVs). Such low respiratory control was most likely due to leaky vesicles. Light scattering experiments indicate that the vesicles had an average diameter of 40 to 70 nm. No evidence for particles in the 4.5–20-nm range was found thus indicating the absence of CcO in a micellar phase. While respiratory control was poor for these vesicles, it was found necessary to utilize purified synthetic lipids to reduce contaminating fluorescence from impurities found in a more conventional vesicular system. Using semi-purified phosphatidylcholine, RCRs > 5 have been obtained using the identical reconstitution procedure.

Fluorescence Quenching

Fluorescence emission spectra of the NCD-4-COVs and COVs were obtained by exciting the sample at 320 nm and scanning from 350 to 550 nm. All bandwidths were 8 nm. 50–200 μl of vesicles were brought to 1 ml with 100 mM pH 7.4 K-Phos and the emission spectra were recorded. Quenchers were added from a stock solution and emission spectra were recorded about

30 s after the addition of quencher. Difference spectra were computed from the fluorescence of NCD-4-COVs and COVs observed under identical conditions to obtain the NCD-4-CcO fluorescence spectra in the absence or presence of quencher. For comparison of NCD-4 quenching efficiencies, spectra were integrated from 400–550 nm.

Various quenchers were used to obtain information about the labeled residue. For example, quenching by membrane impermeant iodide ions and water-soluble TEMPO nitroxides was used to determine exposure of the residue to the aqueous solvent. Quenching by the more hydrophobic *n*-DOXYL-stearic acids was used to indicate location of the fluorescent label with respect to the interior of the membrane bilayer. DOXYL-stearic acids labeled with the nitroxide group at varying locations on the fatty acid chain were used to attempt to pinpoint the depth at which the NCD-4 labeled residue was buried within the bilayer. It is assumed that the DOXYL-stearic acids tend to orient themselves perpendicular to the plane of the bilayer with their carboxyl groups anchored at the bilayer-aqueous interface. The stearic acid acting as the most effective quencher is assumed to have the nitroxide positioned nearest the NCD-4 labeled residue.

Spin-labeled stearic acid stock solutions were made approximately 100 mM in ethanol. First derivative EPR spectroscopy was used to determine the relative concentrations of spin-labels in these stock solutions as follows. First derivative EPR spectra were taken of three different aliquots of all stock solutions. Peak to trough heights of the middle band were assumed to be proportional to the concentration of spin-label and an average height was determined for each of the stearic acid stock solutions. The average height over all spin-labels was assumed to correspond to 100 mM, and this intensity was used to determine the concentration of each spin-label stock solution. We note that in ethanol solution, all of the DOXYL nitroxides used should have similar EPR line widths so the spin concentration can be determined from the height of the central line. The concentration of the 4-amino-TEMPO stock solution was determined by comparison of its EPR signal with that of an accurately made TEMPO stock solution. All spin label solutions were stored at −80°C until use. Potassium iodide solutions were prepared immediately before use. The NCD-4-acetylurea model compound was synthesized by reaction of NCD-4 with acetic acid as described by Chadwick and Thomas (1983).

Data Analysis

Fluorescence quenching by spin-labeled stearic acids has previously been employed to map the location of fluorescent groups in membrane bilayers. Pringle and Taber (1985) used these spin probes to locate the major carbodiimide binding site on the mitochondrial proton channel of the bovine F_0F_1 ATPase. Chatelier et al. (1984) used DOXYL-stearic acids to determine the distribution of tryptophan residues in the purple membranes of *Halobacterium halobium*. The latter investigators noted that the various DOXYL-stearic acids used had different effective partition coefficients for their equilibrium distribution between membrane and aqueous phases. Since it is the concentration of spin-label in the membrane phase that is responsible for the observed quenching of a fluorophore within this phase, it is necessary to determine either the partition coefficient or the concentration of quencher within the membrane phase for each quencher in order to interpret the quenching data in a meaningful way. Toward this end, the quenching of NCD-4-COVs was examined as a function of lipid concentration. These data allow comparison of the quenching by different nitroxides at the same effective concentration of quencher within the membrane phase.

The vesicle solution is best treated as a two-phase system. The partitioning of the quencher between the lipid and aqueous phases is described by:

$$K_p = \frac{A_{Q_L}}{A_{Q_A}} \approx \frac{[Q]_L}{[Q]_A} \tag{1}$$

where A denotes the activity of the quencher in the respective phase, and these activities can be approximated by the concentration of the quencher in the appropriate phase. $[Q]_L = Q_L/V_LM$ and $[Q]_A = Q_A/V_AM$ are the concentrations (e.g., in moles/liter) of quencher in the lipid and aqueous phases, respectively; V_L and V_A are the volumes (e.g., in milliliters) of the respective phases; Q_L and Q_A denote the amount (e.g., in milligrams) of quencher in the two phases; and M is the molecular weight of the quencher. Since the total amount of quencher in an aqueous vesicle solution is $Q_T = [Q]_LV_LM + [Q]_AV_AM$, the overall concentration of quencher is given by:

$$[Q]_T = \frac{Q_T}{V_TM} = [Q]_L\left(\frac{V_L}{V_T}\right) + [Q]_A\left(\frac{V_A}{V_T}\right) \approx [Q]_A + [Q]_L\left(\frac{V_L}{V_T}\right)\left(1 - \frac{1}{K_p}\right) \tag{2}$$

where it is assumed that the volumes are additive, i.e., $V_T \approx V_A + V_L$. This result may be rewritten as:

$$[Q]_T = [Q]_A + \frac{n}{M}[L]\left(1 - \frac{1}{K_p}\right) \tag{3}$$

where $n = Q_L/L$ is the quencher to lipid ratio, L is the amount of lipid in solution (e.g., in milligrams); and $[L] = L/V_T$, i.e., the overall lipid concentration (e.g., in milligrams/ml).

Equation 3 can be used in conjunction with the fluorescence data to provide an estimate of K_p for a given quencher through a comparison of the $[Q]_T$ values required to achieve a given quenching efficiency at various lipid concentrations, $[L]$. It is assumed in this analysis that the measured quenching efficiency (F_0/F) provides a direct measure of $[Q]_L$. As $[L]$ increases, the total amount of quencher ($[Q]_T$) necessary to yield the same observed fluorescence increases. On the other hand, $[Q]_L$ is expected to be the same for identical quenching efficiencies. Similarly, from the partition equilibrium, $[Q]_A$ is expected to be essentially a constant for a given quenching efficiency by a given quencher. Plotting $[Q]_T$ against $[L]$ for a given quenching efficiency according to Eq. 3 therefore should yield a common y-intercept, namely $[Q]_A$, for this value of $[Q]_L$ (n is also essentially a constant for a given $[Q]_L$). After determining $[Q]_A$ in this manner and assuming that $V_A/V_T \approx 1$ (i.e., sufficiently dilute lipid suspensions), one can estimate $[Q]_L$ by rearranging the first equality in Eq. 2:

$$[Q]_L = \frac{V_T}{V_L}[[Q]_T - [Q]_A] \tag{4}$$

The determination of $[Q]_A$ and $[Q]_L$ by this method allows estimation of K_p by Eq. 1. Since it is the concentration of quencher in the lipid, $[Q]_L$, not the total quencher concentration, $[Q]_T$, that determines the observed fluorescence, it is only meaningful to compare the effectiveness of various quenchers at the same $[Q]_L$. For a given concentration of lipid, $[L]$, plotting quenching efficiency against $[Q]_L$ for the different spin-labels yields the information necessary to map the approximate location of the fluorescent probe vis-à-vis the plane of the bilayer. Finally, for a quencher that is preferentially partitioned into the lipid phase, say $K_p \geq 10^4$, $[Q]_T \gg [Q]_A$ if $V_T/V_L < 1000$ in which case $[Q]_L$ may be adequately approximated by $[Q]_L \approx (V_T/V_L)[Q]_T$.

RESULTS

NCD-4 Labeling of CcO

The reaction of NCD-4 with CcO can potentially yield two fluorescent products with overlapping fluorescence spectra, an NCD-4-acylurea and NCD-4-urea (Fig. 1). According to Chadwick and Thomas (1983), the quantum yield of fluorescence of NCD-4-urea is about 10 times greater than that of NCD-4-acylurea (adduct with protein—see Table 1) and therefore interferes with attempts to monitor quenching of the fluorescence from the labeled protein. This problem is accentuated by the fact that a 100-fold molar excess of NCD-4 is required to obtain sufficient labeling of the protein and this excess results in a great deal of the undesired urea. Some of this NCD-4-urea is easily removed since it has a low

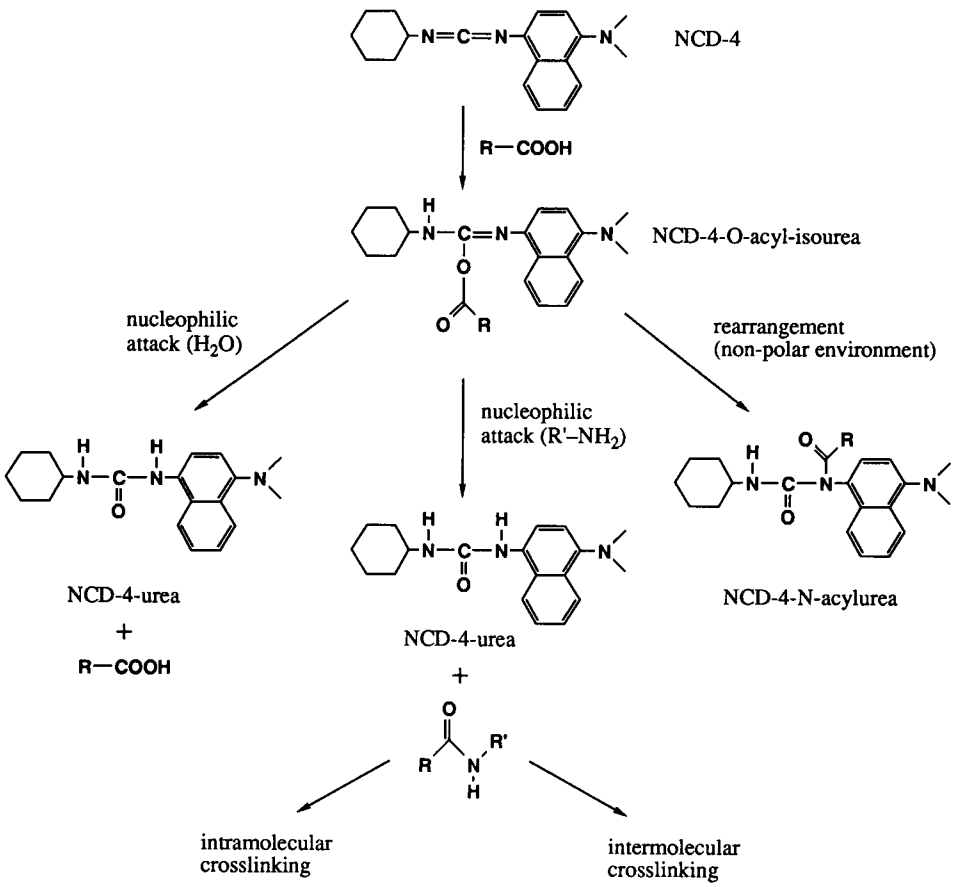

FIGURE 1 Schematic representation of the possible reactions following an initial modification of a single carboxyl group in a protein by NCD-4 (Chadwick and Thomas, 1983; Azzi et al., 1984).

solubility and precipitates out of solution. The remaining NCD-4-urea seems tightly associated with the protein as evidenced by the fact that the residual NCD-4-urea was not removed upon passing the sample through a 1.5 × 15 cm G-100 column. Likewise, there was virtually no loss of the NCD-4-urea upon 16 h dialysis against a 100-fold excess of detergent-buffer (Fig. 2, *a–c*).

On the other hand, almost all of the urea can be removed by applying the protein to a DE-52 or DEAE column and washing with about 200 ml of buffer (low salt) before elution (high salt). EPR spectroscopy reveals, however, that a significant amount of Cu_A is converted to a type-II-like copper (Li et al., 1988) with this purification procedure (EPR data not shown). Decreasing the volume of the wash buffer to about 50 ml limits the modification of Cu_A; however, the removal of the NCD-4-urea is incomplete (see Fig. 2, *d* and *e*). Interestingly, this remaining NCD-4-urea is lost during the formation of vesicles by cholate dialysis. Reconstitution of NCD-4-CcO without any removal of NCD-4-urea by anion exchange chromatography also yields vesicles devoid of the NCD-4-urea impurity. Thus, the anion exchange chromatography step was either omitted or the NCD-4-CcO was washed with only 50 ml buffer on a DEAE column before reconstitution for use in the fluorescence quenching experiments.

SDS-PAGE indicates that NCD-4 labels predominantly subunit III of CcO (Fig. 3). A small amount of fluorescence from subunits I and IV was sometimes observed; this phenomenon depended on preparation of enzyme and was not investigated further. The fluorescence from subunit III always appeared much bluer than that from subunits I and IV which was yellowish; this yellowish fluorescence was similar in color to the tryptophan fluorescence observed from the native subunit I. The modification of subunits I and IV by NCD-4 thus appears minimal.

DCCD inhibition of NCD-4 labeling of CcO

Reaction of CcO with DCCD before incubation with NCD-4 results in reduced NCD-4-acylurea fluorescence per mole of protein. Using samples treated identically except for the amount of DCCD added to the solutions, it was determined that a 100-fold excess of DCCD inhibited NCD-4 labeling by about 53%; a 500-fold excess of DCCD inhibited labeling by about 70%. In order to reduce the interfering NCD-4-urea fluorescence, these samples were washed on a DE-52 column with about 200 ml of low salt buffer before elution and the fluorescence spectra were integrated from 400 to 410 nm. SDS-PAGE reveals that NCD-4 labeling of subunit III is inhibited by DCCD (Fig. 3). A comparison of the fluores-

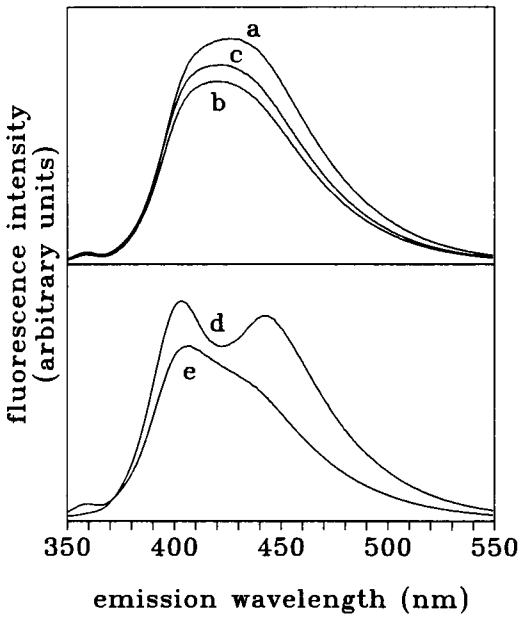

FIGURE 2 Fluorescence spectra of NCD-4-CcO following various levels of purification. (*a*) NCD-4-CcO after a 1.5 × 15 cm G-100 column; (*b*) NCD-4-CcO after a 1.5 × 15 cm G-100 column and 16-h dialysis; (*c*) NCD-4-CcO after two 1.5 × 15 cm G-100 columns and 16-h dialysis; (*d*) NCD-4-CcO after a 50-ml wash on a DEAE column; (*e*) NCD-4-CcO after a 200-ml wash on a DEAE column. The fluorescence maximum of the NCD-4-protein adduct occurs at about 405 nm, and the NCD-4-urea has an emission maximum at about 445 nm. All emission spectra were obtained in 10 mM pH 7.4 K-Phos, 0.1% Brij-35 with excitation wavelength of 320 nm. The small peak at about 360 nm is a Raman band of water.

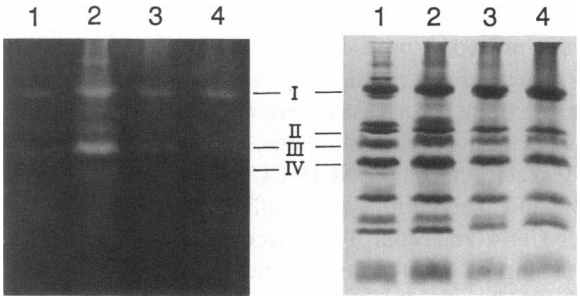

FIGURE 3 SDS-PAGE of NCD-4-CcO: (*left*) fluorescence, (*right*) Coomassie Blue stain. Lane 1, native CcO; lane 2, CcO treated with a 100-fold molar excess of NCD-4; lane 3, CcO treated with a 100-fold molar excess of DCCD before reaction with a 100-fold molar excess of NCD-4; lane 4, CcO treated with a 500-fold molar excess of DCCD before reaction with a 100-fold molar excess of NCD-4. All samples were depleted of NCD-4-urea before electrophoresis by washing with ~ 200 ml low salt buffer on a DE-52 column before elution as described in Materials and Methods (i.e., fluorescence emission spectra of samples like that of Fig. 2 *e*). In each case, there is 168 μg total protein per lane.

cence of subunit III when NCD-4 is reacted with native protein (Fig. 3, lane 2) with the subunit III fluorescence resulting from incubation of NCD-4 with DCCD-inhibited enzyme (lanes 3 and 4) indicates that DCCD almost completely inhibits NCD-4 labeling of CcO. These DCCD inhibition results strongly suggest that NCD-4 and DCCD modify the identical site on CcO; thus, NCD-4 should be effective as a fluorescence probe of the Glu-90 DCCD binding site.

FLUORESCENCE QUENCHING OF NCD-4-COVS

The NCD-4-CcO fluorescence was investigated over the range of quencher concentrations where F_0/F ranged from unity to about 2. F_0 is the fluorescence in the absence of quencher and F is the fluorescence at a given quencher concentration. Quenching is predicted by the Stern-Volmer equation:

$$\frac{F_0}{F} = (1 + k_q\tau_0[Q])(1 + K_a[Q]) \quad (5a)$$

$$\frac{F_0}{F} = (1 + K_{sv}[Q])(1 + K_a[Q]) \quad (5b)$$

where k_q is the bimolecular quenching constant; τ_0 is the fluorescence decay time of the fluorophore in the absence of the quencher; K_{sv} is the dynamic quenching constant; K_a is the static quenching constant; and $[Q]$ is the effective concentration of the quencher. Equation 5 predicts that the observed quenching efficiency is second order with respect to the quencher concentration. Thus, the quenching data were fitted to a second degree polynomial.

The lipids used for the formation of vesicles were not completely devoid of fluorescent impurities; however, the subtraction of a COV spectrum from an NCD-4-COV spectrum obtained under identical conditions should correct for the contribution of these impurities to the emission spectrum (Fig. 4). The DOXYL-stearic acids employed in this study

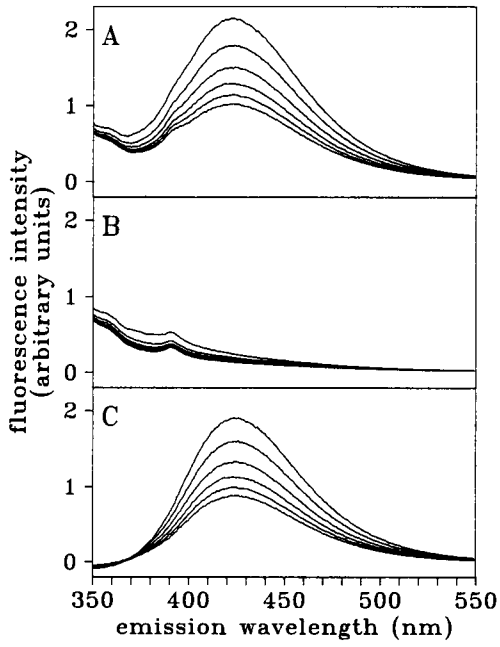

FIGURE 4 Typical fluorescence titration curves of (*A*) NCD-4-COVs and (*B*) COVs with 12-DOXYL-stearic acid as the quencher ($[Q]_T$ = 0–716 μM). The lipid concentration was 2.19 mg/ml. (*C*) depicts the set of difference spectra (*A-B*) used to calculate the quenching efficiencies at the various quencher concentrations.

contain fluorescence impurities as well, but the simple subtraction procedure used should be sufficient also to eliminate any undesired contribution of these impurities to the emission spectrum. In the case of titration with 7-DOXYL-stearic acid at high lipid concentrations, however, subtraction of a COV spectrum from an NCD-4-COV spectrum obtained under identical conditions apparently did not suffice to isolate the NCD-4 emission. The fluorescence maximum in the quenching of NCD-4 fluorescence with 7-DOXYL-stearic acid at $[L]$ = 3.50 mg/ml (as analyzed by the subtraction procedure described) was blue-shifted ~7 nm and the fluorescence peak became distorted toward the red (data not shown). Accordingly, the 7-DOXYL-stearic acid quenching data for $[L]$ = 3.50 mg/ml were not included in the analysis.

A representative plot summarizing the fluorescence quenching of NCD-4-COVs by the DOXYL-stearic acids is shown in Fig. 5 *A*. The data represent quenching by 12-DOXYL-stearic acid at four different lipid (vesicle) concentrations. For each lipid concentration, the data were fitted to a second degree polynomial. Using these best fit curves, the DOXYL-stearic acid concentration that yielded a given F_0/F were estimated for each of the four lipid concentrations studied. The result is the family of curves shown in Fig. 5 *B*, where the total quencher concentration required to achieve a given quenching level is plotted against the four lipid concentrations. According to Eq. 3, the *y*-intercept of each of these curves (corresponding to various quenching efficiencies) is the quencher concentration in the aqueous phase, $[Q]_A$. Using this value for $[Q]_A$ and estimating the lipid density as 1.0 g/cm^3, one can calculate the concentration of quencher in the lipid phase, $[Q]_L$, for a given quenching efficiency according to Eq. 4. Based on these results, one can estimate K_p, i.e., the ratio of $[Q]_L$ to $[Q]_A$ (Eq. 1). It turns out that K_p is on the order of 10^3–10^4, which is sufficiently large that the plots of $[Q]_T$ vs. $[L]$ approach straight lines with n/M) as the slope for a given quenching efficiency (Eq. 3), thus allowing a direct determination of n.

Finally, F_0/F can be replotted against n and the effectiveness of different quenchers can be directly assessed. The results for the various DOXYL-stearic acids utilized in this study are consolidated in Fig. 6 to facilitate this comparison. Summarized here are the results from two completely independent sets of experiments (different starting protein, different vesicle sizes, etc.). These data suggest that 7- and 10-DOXYL-stearic acids are the most effective quenchers

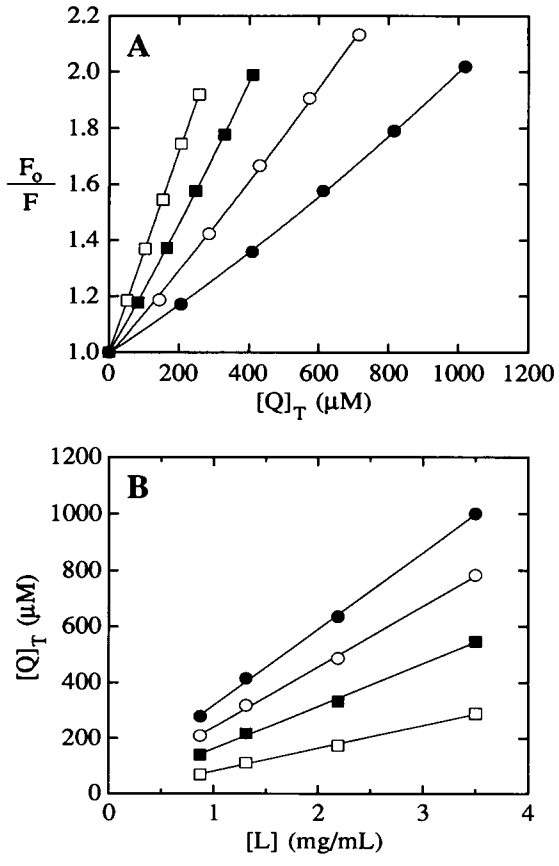

FIGURE 5 (*A*) Quenching efficiency against 12-DOXYL-stearic acid concentration for four different lipid concentrations, [L]: 0.875 (□), 1.31 (■), 2.19 (○), and 3.50 (●) mg/ml. (*B*) The data were replotted according to Eq. 3 after estimating the total 12-DOXYL-stearic acid concentration required to achieve a given quenching efficiency (F_0/F) for the different lipid concentrations: F_0/F = 1.25 (□), 1.50 (■), 1.75 (○), 2.00 (●).

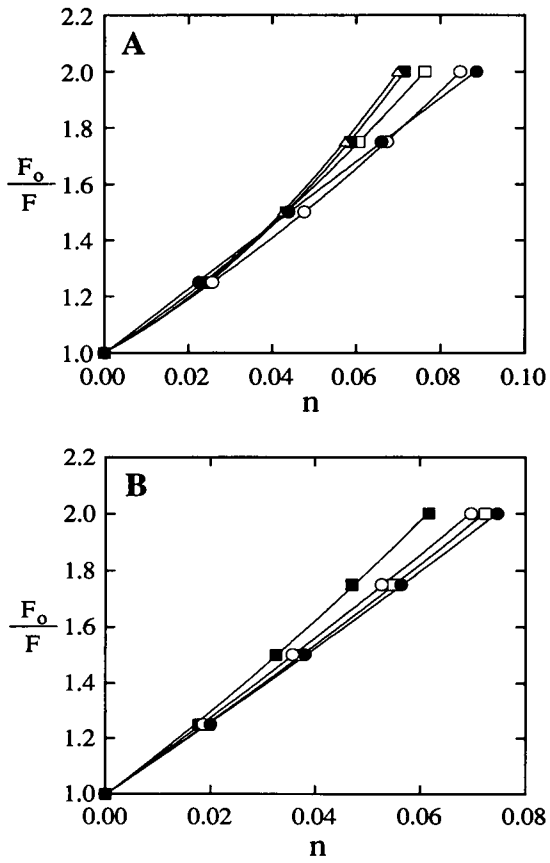

FIGURE 6 Quenching efficiency plotted against n, the quencher/lipid weight ratio, for several different DOXYL-stearic acids. The two plots A and B summarize data obtained from two different sets of experiments: 5-DOXYL (□), 7-DOXYL (■), 10-DOXYL (△), 12-DOXYL (○), 16-DOXYL (●).

and 16-DOXYL-stearic acid is the least effective in quenching the fluorescence of NCD-4-CcO. The inescapable conclusion that one can draw from these data is that the NCD-4 probe is located close to the lipid exposed region of CcO in the modified enzyme.

Since the partition coefficient for the DOXYL-stearic acids is large (10^3–10^4), the bulk of the quencher molecules reside in the lipid phase and $[Q]_A \ll [Q]_T$. Accordingly, a comparison of the various DOXYL quenchers may be made by plotting F_0/F vs. $[Q]_L$ as in Fig. 7, with $[Q]_L$ estimated by $V_T/V_L\,[Q]_T$. Note the similarity between the plots of F_0/F vs. n (Fig. 6) and F_0/F vs. $[Q]_L$ (Fig. 7). In each case, the identical conclusion is reached regarding the location of the NCD-4 probe vis-à-vis the bilayer membrane and the surface of the protein, namely, that the NCD-4 label is located near carbon positions 7–10 of stearic acid.

As controls, the quenching of NCD-4-COVs by KI as well as by two water soluble nitroxides, TEMPO and 4-amino-TEMPO, was also studied. Results from these experiments are summarized in Fig. 8. As expected, the most hydrophobic of the soluble nitroxides (TEMPO) proved to be the most effective quencher and KI was the least effective in quenching of the NCD-4 fluorescence. It may seem somewhat surprising that KI is a more effective quencher of NCD-4-acetylurea in dodecyl-β-D-maltoside micelles rather than in free solution (20% ethanol solution) for one expects the hydrophobic model compound to partition preferentially into the micelle (Fig. 8 *B*). One should be reminded, however, that the sugar moieties of the detergent molecules have a high affinity for iodide ions and hence act to increase the local concentration of the quencher ion. In any case, the KI quenching of NCD-4-acetylurea in dodecyl-β-D-maltoside micelles clearly establishes iodide as an effective quencher for the fluorophore in question. Upon comparison of $[Q]_T$s necessary to yield a given quenching efficiency, it is clear that the DOXYL-stearic acids were more effective in quenching the NCD-4-CcO fluorescence than the TEMPO nitroxides by about one order of magnitude. Note the different abscissa scales for the DOXYL (Fig. 5 *A*), TEMPO (Fig. 8 *A*) and the heavy atom quenchers (Fig. 8 *B*). These results are consistent with the conclusions derived from the DOXYL-stearic acid quenching experiments that the NCD-4 probe in the modified CcO resides at or close to the surface of the protein in the hydrophobic region exposed to the membrane bilayer.

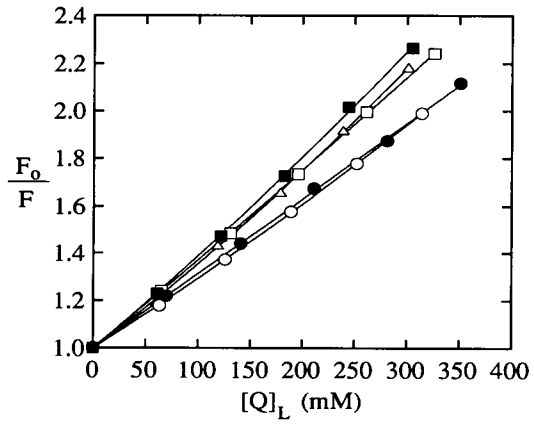

FIGURE 7 Quenching efficiency plotted against $[Q]_L$ for the different DOXYL-stearic acids studied. The lipid concentration was 1.31 mg/ml. The legend is the same as in Fig. 6.

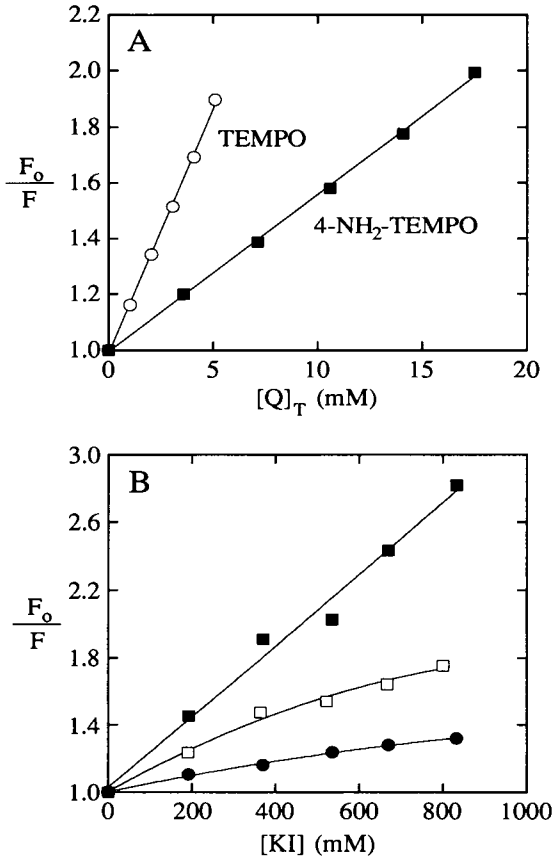

FIGURE 8 (*A*) Quenching of NCD-4-CcO by TEMPO and 4-amino-TEMPO. The lipid concentration was 1.31 mg/ml. (*B*) Comparison of the quenching of NCD-4-CcO and the model compound NCD-4-acetylurea by potassium iodide: (●) NCD-4-CcO ([*L*] = 1.31 mg/ml), (□) NCD-4-acetylurea in ethanol/100 mM pH 7.4 Na-Phos (1:4, v/v), (■) NCD-4-acetylurea in 100 mM pH 7.4 Na-Phos, 0.1% dodecyl-β-D-maltoside.

DISCUSSION

Reaction of NCD-4 with CcO

N-(2,2,6,6-Tetramethylpiperidyl-1-oxyl)-*N'*-cyclohexylcarbodiimide (NCCD), a spin-label analog of DCCD, appears to modify CcO at the DCCD site (Casey et al., 1981a,b), suggesting that NCD-4 would label also at this site. The inhibition of NCD-4 labeling of the enzyme by DCCD confirms this expectation.

In the course of these experiments, it was found that fairly harsh conditions (anion exchange chromatography which tends to modify CcO) were necessary to completely isolate the fluorescently labeled protein from the NCD-4-urea sideproduct. According to Chadwick and Thomas (1983), the

fluorescence maximum of NCD-4-urea can be an effective indicator of the solvent dielectric in the immediate vicinity of this side product. These investigators have reported that NCD-4-urea has a fluorescence maximum at about 460 nm in pure ethanol and at about 473 nm in 50% ethanol (Table 1). The λ_{max} of 445 nm observed for the fluorescence emission of the bound NCD-4-urea (Fig. 2 *d*) indicates that the bound NCD-4-urea must be located in a fairly hydrophobic environment ($\epsilon < 10$).

Glu-90 Resides in a Hydrophobic Environment

Previous work by Casey and co-workers (1981a,b) on NCCD-labeled CcO indicates that the DCCD binding site is fairly apolar. The present study provides two lines of evidence in support of this conclusion. First, the λ_{max} of the fluorescence emission by NCD-4-CcO is consistent with the idea that the NCD-4 probe is located in a hydrophobic environment. Second, the apolar location of the NCD-4 probe is confirmed by the effective quenching of the NCD-4 fluorescence by DOXYL-stearic acids that partition preferentially into the bilayer membrane.

The fluorescence spectrum of NCD-4-CcO reveals that the DCCD-binding site is not exposed to the aqueous solvent. In this study, the fluorescence maximum of NCD-4-CcO never exceeded 425 nm. Chadwick and Thomas (1983) have reported a fluorescence maximum for N-acetylurea of about 398 nm in hexane, 425 nm in ethanol, and 440 nm in 50% ethanol (Table 1). In our hands, the NCD-4-acetylurea model compound has a fluorescence maximum of about 420 nm in dodecyl-β-D-maltoside micelles and 440 nm in 20% ethanol (data not shown). It thus appears that the NCD-4 probe is located in a fairly hydrophobic environment. Interestingly, the detergent (Brij-35) solubilized NCD-4-CcO exhibits a fluorescence maximum at about 405 nm (Fig. 2), though the maximum is around 425 nm (Fig. 4) in the reconstituted protein. This difference in λ_{max} of the emission most likely reflects the different environments surrounding the NCD-4 probe in the detergent solubilized and reconstituted proteins.

It is clear that the different effectiveness of the DOXYL-stearic acids, the TEMPO derivatives and KI in quenching the fluorescence of NCD-4-COVs indicates that the NCD-4 probe is located in a hydrophobic environment. Our aim in using the various DOXYL-stearic acids was to pinpoint the depth at which NCD-4 is embedded within the membrane bilayer. While none of the DOXYL derivatives used is clearly the most effective quencher, the data suggests that the NCD-4 probe resides at a membrane depth near the middle of the hydrocarbon chain of stearic acid in the region near carbon positions 7–10 (Figs. 6 and 7). Our data indicate that 16-DOXYL-stearic acid was the least effective DOXYL quencher. If we assume that the probe is not located in the central region of the membrane (11–16-carbon region of stearic acid) as our data suggest, then the distance between quencher planes of the two leaflets is >10–12 Å. This distance is basically the critical interaction distance indicating that quenching from the opposite leaflet is most likely insignificant. A calculation using the "parallax" method (Abrams and London, 1992) validates these general conclusions. The effectiveness of a given nitroxide as a quencher depends upon the distance of closest approach to the NCD-4 fluorophore, and this distance is constrained by its position on the hydrocarbon chain as the fatty acid anchors itself in the membrane. It is important to point out that the DOXYL-stearic acid quenching data allow determination of the position of the NCD-4 fluorophore, *not* that of Glu-90, within the membrane bilayer. The center of the fluorescent naphthalene moiety of the NCD-4 probe can be as far as ~ 5 Å away from the carboxyl carbon of Glu-90. In any case, it is clear that the NCD-4 label, and by extension Glu-90, is located in a domain of subunit III that is embedded within the lipid milieu. The high concentrations of water soluble quenchers required to quench the NCD-4-CcO fluorescence is consistent with this picture. The effectiveness of 4-amino-TEMPO and TEMPO as quenchers (as manifested by the $[Q]_T$ necessary to achieve a given quenching efficiency) is less by an order of magnitude when compared to the DOXYL-stearic acids (compare Figs. 5 *A* and 8 *A*). If one assumes that both the TEMPO and DOXYL nitroxides have similar intrinsic quenching efficiencies and they affect the observed fluorescence only when they are present in the lipid phase, the partition coefficient for the TEMPO nitroxides is on the order of 10^1–10^2 (compare Figs. 7 and 8 *A*) compared to 10^3–10^4 for the DOXYL-stearic acids. Even higher concentrations of potassium iodide (another two orders of magnitude) are required to achieve comparable quenching as the water-soluble TEMPO nitroxides.

Possible Role of Glu-90 in CcO Function

Since Glu-90 is strictly conserved in all known sequences, it is likely that this residue plays an important role in the function of CcO. Although Glu-90 may not be part of a proton channel as previously suggested, this residue, as well as subunit III, may still have some functional role in the proton pumping function of CcO. At the very least, subunit III can play a structural role (also suggested by Haltia et al. (1991)) as it has been known for some time that the ligand structure of Cu_A in subunit II becomes unstable upon subunit III-depletion (Li et al., 1988). Moreover, subunit III could serve as an allosteric effector and modulate the allosteric interactions between subunits I and II that are expected to be obligatory for redox linkage. One scenario is that these allosteric interactions can be tuned by subunit III to allow modulation of the proton to electron stoichiometry as a function of membrane potential. Since two protons are pumped per electron for the last two electrons of a turnover cycle (Wikström, 1989), it is possible that one proton is pumped in a directly coupled fashion and the second proton is linked to (a) redox center(s) in an indirect fashion (Chan and Li, 1990). Under sufficiently high membrane potential, it is conceivable that the indirect mechanism may become disengaged, and it may be that subunit III is involved here. If there is any truth to this scenario, it predicts that substitution of Glu-90 by site-

directed mutagenesis will merely disrupt the ability of the proton pump to respond to varying energized states of the mitochondrion. This is a testable hypothesis. To date, however, H^+/e^- ratios in proton pumping experiments involving native and mutant CcO have been determined only by extrapolation to zero membrane potential. To explore the modulating effect of subunit III, specifically Glu-90, it is necessary to compare the response of native and mutant CcO as a function of transmembrane potentials in detail. Finally, since exposure of Glu-90, a strictly conserved charged residue, to the interior of the membrane bilayer is extremely unfavorable energetically, it is possible that Glu-90 salt-bridges with one of the two strictly conserved histidines of subunit III (His-204 and His-243—bovine numbering) that are predicted to be part of transmembrane helices on the basis of hydropathy plots (Fig. 9).

CONCLUSIONS

1. In light of these fluorescence results, we conclude that the Glu-90 of subunit III resides near the protein-lipid interface of the membrane spanning region of the enzyme. A proton channel through the protein is expected to be inaccessible from the lipid bilayer and confined, allowing passage of molecules no larger than H_3O^+. Since the interaction distance for fluorescence quenching by nitroxides is 11–15 Å (Abrams and London, 1992) and the diameter of a transmembrane helix is ≥10 Å, it is evident from our results that Glu-90 could be on the interior side of a helix in contact with the lipid bilayer. This situation would allow Glu-90 to be part of a proton channel through the protein. However, the reaction of diimides with Glu-90 would likely disrupt the helix-helix packing and/or reorient the membrane helices to accommodate the bulky label. As there is no experimental evidence for such a major conformational change upon reaction of the enzyme with DCCD or NCD-4, we prefer a scenario in which Glu-90 is exposed to the lipid milieu. If this is the case, Glu-90 is unlikely to be an element of a proton channel associated with the proton pumping machinery of the enzyme. Our results agree with the mutagenesis results of Haltia et al. (1989) which showed that that Glu-90 is not an element of a proton channel and with previous work that established that the DCCD binding site resides in a hydrophobic environment (Casey et al., 1981a,b). However, this is the first study that attempts to three-dimensionally locate Glu-90 and we experimentally validate the placement of Glu-90 in a transmembrane helix based on hydropathy plots (Fig. 9). In addition, we show that Glu-90 is a surface or near-surface residue exposed to the lipid environment.

2. This is the first study utilizing the fluorescence probe NCD-4 to examine the DCCD binding site. It was found that the emission maxima for the detergent-solubilized and reconstituted NCD-4 labeled protein were different likely indicating different conformations in a micellar and bilayer environment. Such conformational modifications may be a consequence of the important role of phospholipids (especially cardiolipin) in enzyme turnover (Abramovitch et al., 1990; Robinson et al., 1990).

3. This is the first report providing evidence for a binding site for a sideproduct of incubation with carbodiimides (in this case, NCD-4-urea). It is likely that NCD-4-urea binds nonspecifically to hydrophobic regions of the enzyme. On the other hand, NCD-4-urea may bind more specifically suggesting a binding site for dicyclohexylurea which may be responsible, in part, for the reduced proton pumping ability of the DCCD treated enzyme. Additional support for this hypothesis comes from the work of Lehninger and coworkers (1985). These investigators found that the proton pumping activity of CcO is partially inhibited *immediately* after addition of DCCD presumably before the enzyme is

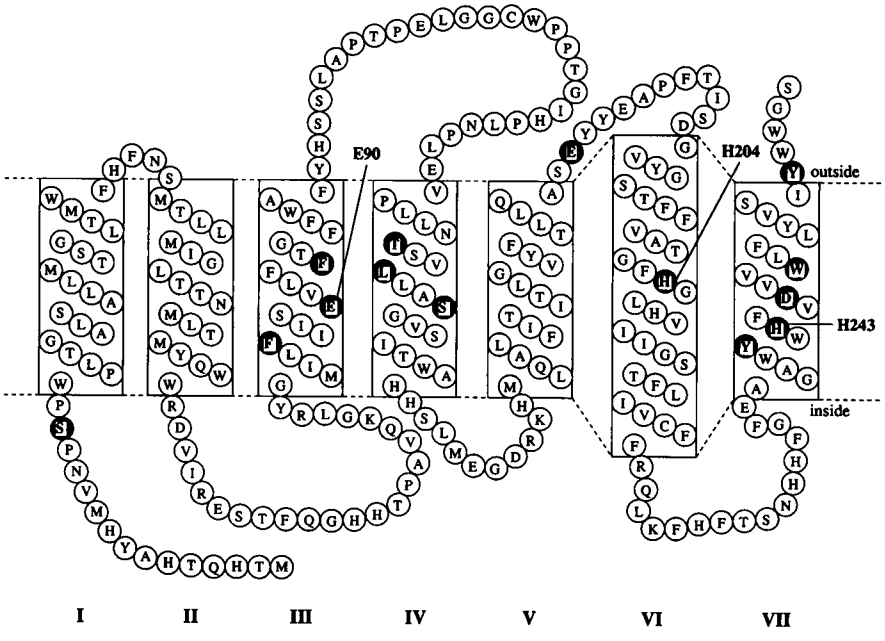

FIGURE 9 Subunit III sequence of bovine heart CcO. Shaded residues are those strictly conserved in 36 cytochrome *c* oxidase subunit III sequences (Mather et al., 1993). Putative transmembrane helices based on hydrophobicity (hydrophobicity scale of Engelman et al. (1986)) are boxed and the cytosolic and matrix sides of the membrane are denoted "outside" and "inside," respectively (Mather et al., 1993). The glutamate residue labeled by DCCD and NCD-4 and the two strictly conserved histidines that could salt-bridge to Glu-90 are labeled.

modified by DCCD at Glu-90 of subunit III suggesting that hydrophobic binding of DCCD may inhibit proton pumping activity.

4. Finally, a novel methodology for interpreting fluorescence quenching results using stearic acid nitroxides is presented. In contrast to previous studies, the resolution of the technique appears poor. This is not due to any theoretical difficulties, but rather arises from the large size of the fluorophore utilized and the large conformational space sampled by the fluorophore. Our conclusion that the NCD-4 probe resides near the protein-lipid interface of the membrane spanning region of the enzyme is firm, however, based on the quenching abilities of water soluble TEMPO derivatives and KI.

This work is supported by grant GM22432 from the National Institute of General Medical Sciences, U. S. Public Health Service. S.M. Musser is the recipient of a National Research Service Predoctoral Award.
Special thanks to Ronald S. Rock for NMR analysis.

REFERENCES

Abramovitch, D. A., D. Marsh, and G. L. Powell. 1990. Activation of beef-heart cytochrome *c* oxidase by cardiolipin and analogs of cardiolipin. *Biochim. Biophys. Acta.* 1020:34–42.

Abrams, F. S., and E. London. 1992. Calibrating the parallax fluorescence quenching method for determination of membrane penetration depth: refinement and comparison of quenching by spin-labeled and brominated lipids. *Biochemistry.* 31:5312–5322.

Azzi, A., R. Bisson, R. P. Casey, H. Gutweniger, C. Montecucco, and M. Thelen. 1979. Hydrophobic interactions, proton movements and dicyclohexylcarbodiimide labeling in cytochrome *c* oxidase. *In* Membrane Bioenergetics. C. P. Lee, G. Schatz, and L. Ernster, editors. Addison-Wesley, Reading, MA. 13–20.

Azzi, A., R. P. Casey, and M. J. Nalecz. 1984. The effect of *N,N'*-dicyclohexylcarbodiimide on enzymes of bioenergetic relevance. *Biochim. Biophys. Acta.* 768:209–226.

Babcock, G. T., and P. M. Callahan. 1983. Redox-linked hydrogen bond strength changes in cytochrome *a*: implications for a cytochrome oxidase proton pump. *Biochemistry.* 22:2314–2319.

Babcock, G. T., and M. Wikström. 1992. Oxygen activation and the conservation of energy in cell respiration. *Nature.* 356:301–309.

Brunori, M., G. Antonini, F. Malatesta, P. Sarti, and M. T. Wilson. 1987. Cytochrome-*c* oxidase: subunit structure and proton pumping. *Eur. J. Biochem.* 169:1–8.

Brunori, M., G. Antonini, A. Colosimo, F. Malatesta, P. Sarti, M. G Jones, and M. T. Wilson. 1985. Stopped-flow studies of cytochrome oxidase reconstituted into liposomes: proton pumping and control of activity. *J. Inorg. Chem.* 23:373–379.

Buse, G., and G. C. M. Steffens. 1991. Cytochrome *c* oxidase in *Paracoccus denitrificans*: protein, chemical, structural, and evolutionary aspects. *J. Bioenerg. Biomembr.* 23:269–289.

Casey, R. P., J. B. Chappell, and A. Azzi. 1979a. Limited-turnover studies on proton translocation in reconstituted cytochrome *c* oxidase-containing vesicles. *Biochem. J.* 182:149–156.

Casey, R. P., M. Thelen, and A. Azzi. 1979b. Dicyclohexylcarbodiimide inhibits proton translocation by cytochrome *c* oxidase. *Biochem. Biophys. Res. Commun.* 87:1044–1051.

Casey, R. P., M. Thelen, and A. Azzi. 1980. Dicyclohexylcarbodiimide binds specifically and covalently to cytochrome *c* oxidase while inhibiting its H^+-translocating activity. *J. Biol. Chem.* 255:3994–4000.

Casey, R. P., C. Broger, M. Thelen, and A. Azzi. 1981. Studies on the molecular basis of H^+ translocation by cytochrome *c* oxidase. *J. Bioenerg. Biomembr.* 13:219–228.

Casey, R. P., C. Broger, and A. Azzi. 1981b. Structural studies on the cytochrome *c* oxidase proton pump using a spin-label probe. *Biochim. Biophys. Acta.* 638:86–93.

Chadwick, C. C., and E. W. Thomas. 1983. Inactivation of sarcoplasmic reticulum ($Ca^{2+}+Mg^{2+}$)-ATPase by *N*-cyclohexyl-*N'*(4-dimethylamino-α-napthyl)carbodiimide. *Biochim. Biophys. Acta.* 730:201–206.

Chan, S. I., and P. M. Li. 1990. Cytochrome *c* oxidase: understanding nature's design of a proton pump. *Biochemistry.* 29:1–12.

Chatelier, R. C., P. J. Rogers, K. P. Ghiggino, and W. H. Sawyer. 1984. The transverse location of tryptophan residues in the purple membranes of *Halobacterium halobium* studied by fluorescence quenching and energy transfer. *Biochim. Biophys. Acta.* 776:75–82.

Engelman, D. M., T. A. Steitz, and A. Goldman. 1986. Identifying nonpolar transmembrane helices in amino acid sequences of membrane proteins. *Ann. Rev. Biophys. Biophys. Chem.* 15:321–353.

Finel, M., and M. Wikström. 1986. Studies on the role of the oligomeric state and subunit III of cytochrome oxidase in proton translocation. *Biochim. Biophys. Acta.* 851:99–108.

Gelles, J., D. F. Blair, and S. I. Chan. 1986. The proton-pumping site of cytochrome *c* oxidase: a model of its structure and mechanism. *Biochim. Biophys. Acta.* 853:205–236.

Green, S. A., D. J. Simpson, G. Zhou, P. S. Ho, and N. V. Blough. 1990. Intramolecular quenching of excited singlet states by stable nitroxide radicals. *J. Am. Chem. Soc.* 112:7337- 7346.

Green, J. A., II, L. A. Singer, and J. H. Parks. 1973. Fluorescence quenching by the stable free radical di-*t*-butylnitroxide. *J. Chem. Phys.* 58: 2690–2695.

Haltia, T., M. Finel, N. Harms, T. Nakari, M. Raitio, M. Wikström, and M. Saraste. 1989. Deletion of the gene for subunit III leads to defective assembly of bacterial cytochrome oxidase. *EMBO J.* 8:3571–3579.

Haltia, T., M. Saraste, and M. Wikström. 1991. Subunit III of cytochrome *c* oxidase is not involved in proton translocation: a site-directed mutagenesis study. *EMBO J.* 10:2015–2021.

Hartzell, C. R., and H. Beinert. 1974. Components of cytochrome *c* oxidase detectable by EPR spectroscopy. *Biochim. Biophys. Acta.* 368:318–338.

Hinkle, P. C., J. J. Kim, and E. Racker. 1972. Ion transport and respiratory control in vesicles formed from cytochrome oxidase and phospholipids. *J. Biol. Chem.* 247:1338–1342.

Kadenbach, B., A. Stroh, F.-J. Hüther, A. Reimann, and D. Steverding. 1991. Evolutionary aspects of cytochrome *c* oxidase. *J. Bioenerg. Biomembr.* 23:321–334.

Larsen, R. W., L.-P. Pan, S. M. Musser, Z. Li, and S. I. Chan. 1992. Could Cu_B be the site of redox linkage in cytochrome *c* oxidase? *Proc. Natl. Acad. Sci. USA.* 89:723–727.

Lehninger, A. L., B. Reynafarje, and L. Costa. 1985. Action of DCCD on the H^+/O stoichiometry of mitoplast cytochrome *c* oxidase. *J. Inorg. Chem.* 23:335–340.

Li, P. M., J. E. Morgan, T. Nilsson, M. Ma, and S. I. Chan. 1988. Heat treatment of cytochrome *c* oxidase perturbs the Cu_A site and affects proton pumping behavior. *Biochemistry.* 27:7538–7546.

Malmström, B. G. 1990. Cytochrome *c* oxidase as a redox-linked proton pump. *Chem. Rev.* 90:1247–1260.

Mather, M. W., P. Springer, S. Hensel, G. Buse, and J. A. Fee. 1993. Cytochrome oxidase genes from *Thermus thermophilus*: nucleotide sequence of the fused gene and analysis of the deduced primary structures for subunits I and III of cytochrome caa_3. *J. Biol. Chem.* 268:5395–5408.

Matko, J, K. Ohki, and M. Edidin. 1992. Luminescence quenching by nitroxide spin labels in aqueous solution: studies on the mechanism of quenching. *Biochemistry.* 31:703–711.

Mitchell, P. 1987. A new redox loop formality involving metal-catalysed hydroxide-ion translocation: a hypothetical Cu loop mechanism for cytochrome oxidase. *FEBS Lett.* 222:235–245.

Mitchell, P. 1988. Possible protonmotive osmochemistry in cytochrome oxidase. *Ann. NY Acad. Sci.* 550:185–198.

Mitchell, P., R. Mitchell, A. J. Moody, I. C. West, H. Baum, and J. M. Wrigglesworth. 1985. Chemiosmotic coupling in cytochrome oxidase: possible protonmotive O loop and O cycle mechanisms. *FEBS Lett.* 188: 1–7.

Müller, M., and A. Azzi. 1991. Cytochrome *c* oxidase metal centers: location and function. *J. Bioenerg. Biomembr.* 23:291–302.

Pringle, M. J., and M. Taber. 1985. Fluorescent analogs of *N,N'*-dicyclohexylcarbodiimide as structural probes of the bovine mitochondrial proton channel. *Biochemistry.* 24:7366- 7371.

Prochaska, L. J., and P. S. Fink. 1987. On the role of subunit III in proton

translocation in cytochrome *c* oxidase. *J. Bioenerg. Biomembr.* 19: 143–166.

Prochaska, L. J., and K. A. Reynolds. 1986. Characterization of electron-transfer and proton-translocation activities in bovine heart mitochondrial cytochrome *c* oxidase deficient in subunit III. *Biochemistry.* 25:781–787.

Prochaska, L. J., R. Bisson, R. A. Capaldi, G. C. M. Steffens, and G. Buse. 1981. Inhibition of cytochrome *c* oxidase function by dicyclohexylcarbodiimide. *Biochim. Biophys. Acta.* 637:360–373.

Proteau, G., J. M. Wrigglesworth, and P. Nicholls. 1983. Protonmotive functions of cytochrome *c* oxidase in reconstituted vesicles: influence of turnover rate on 'proton translocation.' *Biochem. J.* 210:199–205.

Püttner, I., E. Carafoli, and F. Malatesta. 1985. Spectroscopic and functional properties of subunit III-depleted cytochrome oxidase. *J. Biol. Chem.* 260:3719–3723.

Robinson, N. C., J. Zborowski, and L. H. Talbert. 1990. Cardiolipin-depleted bovine heart cytochrome *c* oxidase: binding stoichiometry and affinity for cardiolipin derivatives. *Biochemistry* 29:8962–8969.

Saraste, M. 1990. Structural features of cytochrome oxidase. *Q. Rev. Biophys.* 23:331–366.

Sarti, P., M. G. Jones, G. Antonini, F. Malatesta, A. Colosimo, M. T. Wilson, and M. Brunori. 1985. Kinetics of redox-linked proton pumping activity of native and subunit III-depleted cytochrome *c* oxidase: a stopped-flow investigation. *Proc. Natl. Acad. Sci. USA.* 82:4876–4880.

Sigel, E., and E. Carafoli. 1980. Quantitative analysis of the proton and charge stoichiometry of cytochrome *c* oxidase from beef heart reconstituted into phospholipid vesicles. *Eur. J. Biochem.* 111:299–306.

Thelen, M., P. O'Shea, G. Petrone, and A. Azzi. 1985. Proton translocation by a native and subunit-III-depleted cytochrome *c* oxidase reconstituted into phospholipid vesicles: use of fluorescein-phosphatidylethanolamine as an intravesicular pH indicator. *J. Biol. Chem.* 260:3626–3631.

Thompson, D. A., L. Gregory, and S. Ferguson-Miller. 1985. Cytochrome *c* oxidase depleted of subunit III: proton-pumping, respiratory control, and pH dependence of the midpoint potential of cytochrome *a*. *J. Inorg. Chem.* 23:357–364.

van Verseveld, H. W., K. Krab, and A. H. Stouthamer. 1981. Proton pump coupled to cytochrome *c* oxidase in *Paracoccus denitrificans*. *Biochim. Biophys. Acta.* 635:525–534.

Wikström, M. 1977. Proton pump coupled to cytochrome *c* oxidase in mitochondria. *Nature.* 266:271–273.

Wikström, M. 1988. How does cytochrome oxidase pump protons? *Ann. NY Acad. Sci.* 550:199–206.

Wikström, M. 1989. Identification of the electron transfers in cytochrome oxidase that are coupled to proton-pumping. *Nature.* 338:776–778.

Wikström, M., and R. P. Casey. 1985. What is the essential proton-translocating molecular machinery in cytochrome oxidase? *J. Inorg. Biochem.* 23:327–334.

Woodruff, W. H., Ó. Einarsdóttir, R. B. Dyer, K. A. Bagley, G. Palmer, S. J. Atherton, R. A. Goldbeck, T. D. Dawes, and D. S. Kliger. 1991. Nature and functional implications of the cytochrome a_3 transients after photodissociation of CO-cytochrome oxidase. *Proc. Natl. Acad. Sci. USA.* 88: 2588–2592.